Inorg. Chem. **2006**, *45*, 1228−1234

Has AuF_7 Been Made?

Sebastian Riedel and Martin Kaupp*

Institut für Anorganische Chemie, Universität Würzburg, Am Hubland, 97074 Würzburg, Germany

Received November 10, 2005

Quantum chemical calculations at DFT (BP86, B3LYP, BHLYP), MP2, CCSD, and CCSD(T) levels have been carried out on various fluoro complexes of gold in oxidation states +V through +VII to evaluate the previously claimed existence of AuF_7. The calculations indicate clearly that elimination of F_2 from AuF_7 is a strongly exothermic reaction with a low activation barrier. This is inconsistent with the reported stability of AuF_7 up to room temperature. A reported experimental vibrational frequency at 734 cm^{-1} for AuF_7 could not be verified computationally. It is concluded that the reported observation of AuF_7 was probably erroneous. As the calculations indicate also an extremely large electron affinity and little stability for AuF_6, Au^V remains the highest well-established gold oxidation state.

1. Introduction

Pushing the known oxidation states for a main group element or transition metal to the highest possible values is often achieved by utilizing fluorine or oxygen ligands because of their small size and high electronegativity. The highest oxidation states for the late transition elements are known for their fluorides (e.g. in the case of IrF_6,[1] RhF_6,[2] or PtF_6;[3,4] claims for high oxidation states in compounds with less electronegative ligands often do not stand up to closer scrutinity of the bonding situation, as in a recent case of a Pd^{VI} complex with supposedly six silyl ligands[5−8]). In the case of gold, the highest oxidation state that is experimentally known beyond doubt is Au^V in the form of various salts of the $[AuF_6]^{-1}$ anion,[9] and as $[AuF_5]_2$.[10,11] Indeed, the pronounced instability of the monofluoride AuF, which has been obtained only relatively recently, is related to the relativistic destabilization of the lower +I relative to the higher +III oxidation state in the presence of electronegative ligands.[12−14] For similar reasons, ongoing speculations about mercury or element 112 in oxidation state +IV concentrate on the tetrafluorides or on closely related species with very electronegative ligands.[15−19]

Could gold be oxidized even beyond the +V oxidation state? Almost 20 years ago, the isolation of AuF_7 was claimed, on the basis of the reaction of solid AuF_5 with atomic fluorine in a vacuum (cf. eq 1), followed by condensation of the reaction products at liquid-nitrogen temperature, and measurement of their IR and molecular weight data.[20,21] AuF_7 was described as a volatile substance that is stable at room temperature but decomposes at 100 °C. However, these claims have never been substantiated or refuted by other groups, although the observed ready

* To whom correspondence should be addressed. Fax: (+49) 931-888-7135. E-mail: kaupp@mail.uni-wuerzburg.de.

(1) Claassen, H. H.; Weinstock, B. *J. Chem. Phys.* **1960**, *33*, 436−437.
(2) Chernick, C. L.; Claassen, H. H.; Weinstock, B. *J. Am. Chem. Soc.* **1961**, *83*, 3165−3166.
(3) Weinstock, B.; Claassen, H. H.; Malm, J. G. *J. Am. Chem. Soc.* **1957**, *79*, 5832.
(4) Wesendrup, R.; Schwerdtfeger, P. *Inorg. Chem.* **2001**, *40*, 3351−3354.
(5) Chen, W.; Shimada, S.; Tanaka, M. *Science* **2002**, *295*, 308−310.
(6) Crabtree, R. H. *Science* **2002**, *295*, 288−289.
(7) Aullon, G.; Lledos, A.; Alvarez, S. *Angew. Chem., Int. Ed.* **2002**, *41*, 1956−1959.
(8) Sherer, E. C.; Kinsinger, C. R.; Kormos, B. L.; Thompson, J. D.; Cramer, C. J. *Angew. Chem., Int. Ed.* **2002**, *41*, 1953−1956.
(9) Mohr, F. *Gold Bull. (London)* **2004**, *37*, 164−169.
(10) Hwang, I.-C.; Seppelt, K. *Angew. Chem., Int. Ed.* **2001**, *40*, 3690−3693.
(11) Brunvoll, J.; Ischenko, A. A.; Ivanov, A. A.; Romanov, G. V.; Sokolov, V. B.; Spiridonov, V. P.; Strand, T. G. *Acta Chem Scand.* **1982**, *A36*, 705−709.
(12) Schwerdtfeger, P. *J. Am. Chem. Soc.* **1989**, *111*, 7261−7262.
(13) Schwerdtfeger, P.; Boyd, P. D. W.; Brienne, S.; Burrell, A. K. *Inorg. Chem.* **1992**, *31*, 3411−3422.
(14) Schwarz, H. *Angew. Chem., Int. Ed.* **2003**, *42*, 4442−4454.
(15) Kaupp, M.; von Schnering, H. G. *Angew. Chem.* **1993**, *105*, 952−954; *Angew. Chem., Int. Ed. Engl.* **1993**, *32*, 861−993.
(16) Kaupp, M.; Dolg, M.; Stoll, H.; von Schnering, H. G. *Inorg. Chem.* **1994**, *33*, 2122−2131.
(17) Seth, M.; Schwerdtfeger, P.; Dolg, M. *J. Chem. Phys.* **1997**, *106*, 3623−3632.
(18) Riedel, S.; Straka, M.; Kaupp, M. *Phys. Chem. Chem. Phys.* **2004**, *6*, 1122−1127.
(19) Riedel, S.; Straka, M.; Kaupp, M. *Chem.—Eur. J.* **2005**, *11*, 2743−2755.
(20) Timakov, A. A.; Prusakov, V. N.; Drobyshevskii, Y. V. *Dokl. Akad. Nauk SSSR* **1986**, *291*, 125−128 [Chem].
(21) Ostropikov, V. V.; Rakov, E. G. *Izv. Vyssh. Uchebn. Zaved., Khim. Khim. Tekhnol.* **1989**, *32*, 3−17.

10.1021/ic051944y CCC: $33.50
Published on Web 01/05/2006

decomposition of $[KrF]^+[AuF_6]^-$ into AuF_5 and F_2 may be viewed as a strong indication of the instability of AuF_7.[22] Even the known 5d hexafluorides range only up to platinum and do not encompass gold. It is not clear why the maximum oxidation state should be higher for Au than for Pt. A theoretical study on AuF_6^{q-} ($q = 0, 1, 2, 3$) species identified the AuF_6^- anion as the preferred minimum with respect to molecular charge q.[23] AuF_6 has been estimated to have an enormous adiabatic electron affinity of about 9.5−10.5 eV.[23−25] This sheds some doubt on the existence of gold oxidation states beyond +V and on the feasibility of the route describd by eq 1. Nevertheless, AuF_7 is sometimes mentioned in the literature as established Au^{VII} species.[26]

$$AuF_5(s) + F(g) \rightarrow AuF_6(g)$$
$$2AuF_6(g) \rightarrow AuF_7(g) + AuF_5(s) \qquad (1)$$

Here we approach the question of the existence of oxidation states Au^{VI} and Au^{VII} by state-of-the-art quantum-chemical calculations.

2. Computational Methods

Calculations have been performed at various levels of density functional theory (DFT) and at ab initio levels up to CCSD(T). For the HF, MP2, and DFT calculations, we used the Gaussian03[27] program and the analytical gradient methods implemented therein. The gradient-corrected BP86[28,29] functional, the hybrid functionals B3LYP[27] (based on the work of Becke)[30] with 20% HF exchange admixture, and the "half-and-half" hybrid functional[27,31] with 50% HF exchange (in the following abbreviated BHLYP) were used. This selection of functionals was chosen on purpose, as our experience with similar high-oxidation-state species taught us that the thermochemistry of the redox reactions of such complexes depends crucially on the amount of the exact-exchange admixture. Coupled-cluster calculations with single and double substitutions (CCSD), as well as with inclusion of perturbative triple excitations [CCSD(T) level] were carried out with the MOLPRO 2002.6[32] program package. All species have been fully optimized at a given computational level, except for some transition states, where coupled-cluster single-point energies were computed at various DFT-optimized structures.

Scalar relativistic effects for gold and platinum were included by a quasirelativistic energy-adjusted, small-core pseudopotential (effective-core potential, ECP).[33] The corresponding (8s6p5d)/[7s3p4d] valence basis set was augmented by two f-type polarization functions. The diffuse function ($\alpha = 0.2$) maximizes the static polarizability, and the compact f function ($\alpha = 1.0$) improves the description of the primary covalent bonding to the metal.[34] Calculations for the present systems without these two f functions led to ca. 2 pm larger bond lengths (data not shown). The fluorine atom was described by an all-electron (9s5p1sp1d)/[4s2p1sp1d]-Dunning-DZ+P[35] basis set.

Basis-set superposition errors (BSSE) were evaluated by counterpoise (CP)[36,37] corrections at optimized structures. Zero-point vibrational energy (ZPE) corrections were computed at DFT and ab initio levels up to MP2. Spin−orbit (SO) coupling was neglected. On the basis of our own experience for mercury fluorides[16] and the results of other groups for gold complexes,[38] SO effects are expected to influence reaction energies involving only closed-shell species negligibly. In the case of the open-shell AuF_6, we cannot exclude completely some influence of SO effects but, as they come mainly from the 5d shell, they should not yet be too dramatic either.

3. Results and Discussion

Structures of Au^{+V}, Au^{+VI}, and Au^{+VII} Fluorides. Structural data for various species are compared in Tables 1 and 2, and some structures are shown in Figures 1−4. For d^6 Au^{+V}, we have considered monomeric AuF_5, $[AuF_6]^-$, the dimer $[AuF_5]_2$, and the trimer $[AuF_5]_3$. Before going into the comparison between theory and experiment for individual molecules, it is appropriate to note that comparison of our B3LYP results with relativistic Au ECP provide generally about 4−5 pm shorter bond lengths than comparative calculations with a nonrelativistic ECP (last column in Table 1).

Our calculations for the AuF_5 monomer indicate a square pyramidal (C_{4v}) minimum (Table 1, Figure 1a), which may scramble its fluorine atoms easily via a trigonal bipyramidal transition state at 9.5 kJ mol^{-1} (B3LYP level). We note in passing that BP86 calculations gave a slight puckering of the fluorine ligands in the basal plane of the square-pyramidal minimum structure, with only a marginal stabilization of 3.4 kJ mol^{-1} relative to the C_{4v} structure (see Supporting

(22) Lehmann, J. F.; Schrobilgen, G. J. *J. Fluorine Chem.* **2003**, *119*, 109−124.
(23) Miyoshi, E.; Sakai, Y. *J. Chem. Phys.* **1988**, *89*, 7363−7366.
(24) Compton, R. N.; Reinhardt, P. W.; Cooper, C. D. *J. Chem. Phys.* **1978**, *68*, 2023−2036.
(25) Compton, R. N.; Reinhardt, P. W. *J. Chem. Phys.* **1980**, *72*, 4655−4656.
(26) (a) Cotton, S. *Chemistry of Precious Metals*; Chapman & Hall: Weinheim, Germany, 1997. (b) Schmidbaur, H. *Gold: Progress in Chemistry, Biochemistry and Technology*; Wiley: New York, 1999.
(27) Frisch, M. J.; Trucks, G. W.; Schlegel, H. B.; Scuseria, G. E.; Robb, M. A.; Cheeseman, J. R.; Montgomery, J. A.; Vreven, J. T.; Kudin, K. N.; Burant, J. C.; Millam, J. M.; Iyengar, S. S.; Tomasi, J.; Barone, V.; Mennucci, B.; Cossi, M.; Scalmani, G.; Rega, N.; Petersson, G. A.; Nakatsuji, H.; Hada, M.; Ehara, M.; Toyota, K.; Fukuda, R.; Hasegawa, J.; Ishida, M.; Nakajima, T.; Honda, Y.; Kitao, O.; Nakai, H.; Klene, M.; Li, X.; Knox, J. E.; Hratchian, H. P.; Cross, J. B.; Adamo, C.; Jaramillo, J.; Gomperts, R.; Stratmann, R. E.; Yazyev, O.; Austin, A. J.; Cammi, R.; Pomelli, C.; Ochterski, J. W.; Ayala, P. Y.; Morokuma, K.; Voth, G. A.; Salvador, P.; Dannenberg, J. J.; Zakrzewski, V. G.; Dapprich, S.; Daniels, A. D.; Strain, M. C.; Farkas, O.; Malick, D. K.; Rabuck, A. D.; Raghavachari, K.; Foresman, J. B.; Ortiz, J. V.; Cui, Q.; Baboul, A. G.; Clifford, S.; Cioslowski, J.; Stefanov, B. B.; Liu, G.; Liashenko, A.; Piskorz, P.; Komaromi, I.; Martin, R. L.; Fox, D. J.; Keith, T.; Al-Laham, M. A.; Peng, C. Y.; Nanayakkara, A.; Challacombe, M.; Gill, P. M. W.; Johnson, B.; Chen, W.; Wong, M. W.; Gonzalez, C.; Pople, J. A. *Gaussian*, revision B.04; Gaussian Inc.: Pittsburgh, PA, 2003.
(28) Becke, A. D. *Phys. Rev. A* **1988**, *38*, 3098−3100.
(29) Perdew, J. P. *Phys. Rev. B* **1986**, *33*, 8822−8824.
(30) Becke, A. D. *J. Chem. Phys.* **1993**, *98*, 5648−5652.
(31) Becke, A. D. *J. Chem. Phys.* **1993**, *98*, 1372−1377.
(32) Werner, H.-J.; Knowles, P. J.; Lindh, R.; Schütz, M.; Celani, P.; Korona, T.; Manby, F. R.; Rauhut, G.; Amos, R. D.; Bernhardsson, A.; Berning, A.; Cooper, D. L.; Deegan, M. J. O.; Dobbyn, A. J.; Eckert, F.; Hampel, C.; Hetzer, G.; Lloyd, A. W.; McNicholas, S. J.; Meyer, W.; Mura, M. E.; Nicklass, A.; Palmieri, P.; Pitzer, R.; Schumann, U.; Stoll, H.; Stone, A. J.; Tarroni, R.; Thorsteinsson, T. *MOLPRO*, version 2002.6; University of Birmingham: Birmingham, U.K., 2003.
(33) Schwerdtfeger, P.; Dolg, M.; Schwarz, W. H. E.; Bowmaker, G. A.; Boyd, P. D. W. *J. Chem. Phys.* **1989**, *91*, 1762−1774.
(34) Pyykkö, P. *Angew. Chem., Int. Ed.* **2004**, *43*, 4412−4456.
(35) Dunning, T. H., Jr. *J. Chem. Phys.* **1970**, *53*, 2823−2833.
(36) Boys, S. F.; Bernardi, F. *Mol. Phys.* **1970**, *19*, 553.
(37) Simon, S.; Duran, M.; Dannenberg, J. J. *J. Chem. Phys.* **1996**, *105*, 11024−11031.
(38) Liu, W.; van Wullen, C. *J. Chem. Phys.* **1999**, *110*, 3730−3735.

Table 1. Optimized Minimum Structures of AuF_5, $[AuF_6]^{-1}$, AuF_6, and AuF_7 [a]

species	HF	MP2	CCSD	CCSD(T)	BP86[b]	BHLYP	B3LYP	*nrel.* B3LYP[c]
				AuF_5 (C_{4v})				
$Au-F_{ax}$	180.5	188.8	186.7	189.0	192.2	183.7	188.2	193.9
$Au-F_{eq}$	185.8	193.0	190.5	192.3	193.5 (193.9)	188.4	192.1	196.2
$\angle(F_{ax}-Au-F_{eq})$	92.3	92.7	92.5	92.7	85.4 (106.7)	92.9	94.0	93.5
T_1 diagnostic			0.0209	0.0213				
				$[AuF_6]^{-1}$ (O_h)				
Au−F	187.1	194.3	191.6	193.2	195.8	189.9	193.9	198.1
T_1 diagnostic			0.0186	0.0188				
				AuF_6 (D_{2h})				
$Au-F_{ax}$	182.1	184.1			192.5		189.9	
$Au-F_{eq}$	186.0	194.7			193.3		191.1	
$\angle(F_{ax}-Au-F_{eq})$	90.0	90.0			90.0		90.0	
$\angle(F_{eq}-Au-F_{eq})$	90.6 (89.4)	90.7 (89.3)			89.6 (90.4)		90.5 (89.5)	
T_1 diagnostic								
				AuF_7 (D_{5h})				
$Au-F_{ax}$	186.1	195.5	191.3	194.4	195.3	189.2	193.4	197.2
$Au-F_{eq}$	188.9	196.4	194.1	197.3	196.3−196.7	191.2	194.7	199.6
T_1 diagnostic			0.0184	0.0189				

[a] Distances in pm; angles in degrees. Different T_1 diagnostics reflect the slight differences in the CCSD and CCSD(T) structures. [b] BP86 structures exhibit lower symmetry for AuF_5 and AuF_7 because of puckering in the basal plane (cf. text). [c] Calculations with a nonrelativistic ECP on gold.

Table 2. Experimental and Computed Structure Parameters for $[AuF_5]_2$ in D_{2h} Symmetry[a]

$[AuF_5]_2$	crystal structure[b]	electron diffraction[c]	MP2[b]	MP2	BP86	B3LYP	BHLYP
Au−F1, Au−F4	189.1(6), 190.1(5)	188.9(9)	196.5	193.8	194.4	192.5	188.7
Au−F2, Au−F3	210.3(5), 203.1(5)	203.0 (7)	207.7	203.9	207.7	206.0	202.4
Au−F5, Au−F6	185.4(6), 187.5(6)	182.2(8)	192.5	190.0	190.4	188.4	184.6
F2−Au−F3	78.4(2)	80.1(5)	79.0	81.4	78.8	78.0	77.4
F1−Au−F4	178.5(3)	181.0(11)	179.3	179.1	178.3	178.7	178.9
F5−Au−F6	87.0(3)	92.3(17)	96.2	88.2	89.2	88.8	88.4

[a] Distances in pm; angles in degrees. [b] Ref 10. [c] Ref 11.

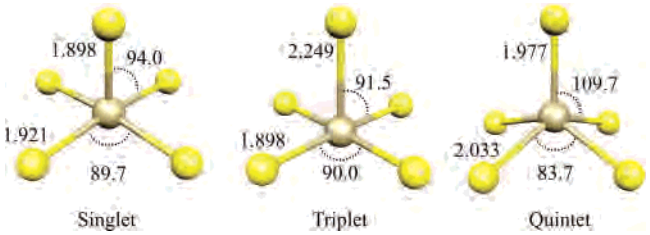

Figure 1. B3LYP-optimized structures for ground and excited states of AuF_5: (a) singlet ground state, (b) lowest-triplet excited state, and (c) lowest-quintet excited state. All three states exhibit C_{4v} minima on their potential energy surfaces (cf. text).

Information for Cartesian coordinates at various levels). As expected, the $[AuF_6]^-$ anion exhibits an octahedral (O_h) minimum with an Au−F distance of 193.9 pm at the B3LYP level, see Table 1. Experimentally determined distances in the solid state are somewhat shorter, between 185 and 190 pm (with deviations from those of an ideal octahedron because of interactions with the countercations).[10,22,26,39−41]

AuF_5 is experimentally produced by thermal decomposition of $[KrF]^+[AuF_6]-$ or $[O_2]^+[AuF_6]^-$.[42,43] Seppelt et al.[10] showed that it prefers to crystallize as the $[AuF_5]_2$ dimer (D_{2h} symmetry) with two bridging fluorine atoms (see Figure 2a). Even in a gas-phase electron diffraction experiment at a nozzle temperature of ca. 220 °C, the dimer was the predominant species, and only a small amount of trimer with presumed D_{3h} structure was present.[11] The computed structure parameters for the dimer agree well with the available X-ray and electron-diffraction measurements (see Table 2, Figure 2a). Similar to earlier comparisons of coupled-cluster and DFT optimizations for mercury(IV) complexes, the shorter bond lengths obtained with the larger HF exchange admixture at the BHLYP level appear to be more reliable. Our B3LYP optimized structure of the trimer shows a slight bending of the Au−F−Au bridges, leading only to C_{3v} symmetry (see Figure 2b).

In addition to the ground-state singlet of AuF_5, we have also optimized the lowest triplet and quintet states. At the B3LYP level, their optimized structures are 5 kJ mol^{-1} and 173 kJ mol^{-1}, respectively, above the singlet ground-state minimum. Figure 1b shows that excitation to the low-lying triplet breaks essentially the axial Au−F bond. This indicates already a lability of the monomeric fluoride. In the higher-lying quintet state (Figure 1c), all bonds are expanded. A B3LYP optimization for triplet $[AuF_5]_2$ gave a minimum 113.6 kJ mol^{-1} above the singlet minimum (Figure 2b), consistent with the enhanced stability of the singlet ground state by dimerization.

Turning to oxidation state +VI, we have looked at the lowest-lying electronic states of the open-shell AuF_6 molecule (d^5 configuration). Both the low-spin doublet (D_{2h} symmetry) and the high-spin sextet (O_h) are minima on their respective

(39) Graudejus, O.; Wilkinson, A. P.; Chacon, L. C.; Bartlett, N. *Inorg. Chem.* **2000**, *39*, 2794−2800.
(40) Leary, K.; Zalkin, A.; Bartlett, N. *J. Chem. Soc., Chem. Commun.* **1973**, 131−132.
(41) Leary, K.; Zalkin, A.; Bartlett, N. *Inorg. Chem.* **1974**, *13*, 775−779.
(42) Holloway, J. H.; Schrobilgen, G. J. *J. Chem. Soc., Chem. Commun.* **1975**, 623−624.
(43) Vasile, M. J.; Richardson, T. J.; Stevie, F. A.; Falconer, W. E. *J. Chem. Soc., Dalton Trans.* **1976**, 351−353.

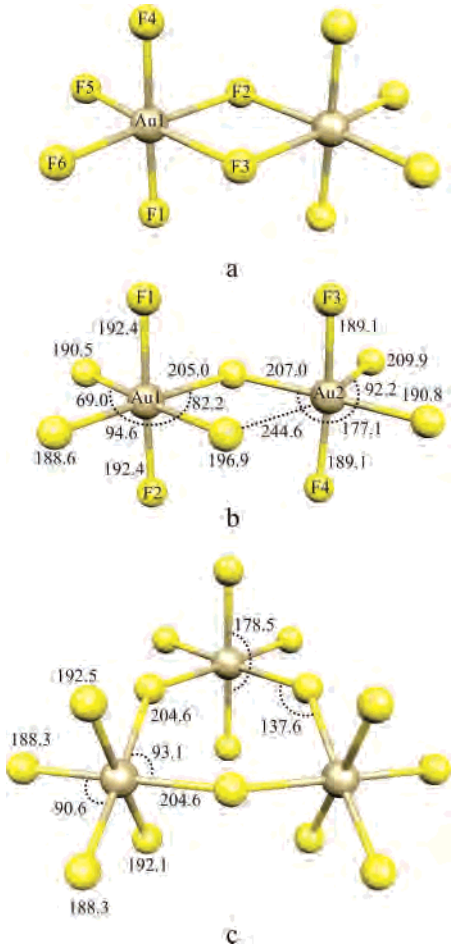

Figure 2. B3LYP-optimized structures for (a) singlet $[AuF_5]_2$ (D_{2h}), (b) triplet $[AuF_5]_2$ (F1−Au1−F2 = 177.6, F3−Au2−F4 = 170.9), and (c) $[AuF_5]_3$ (C_{3v}).

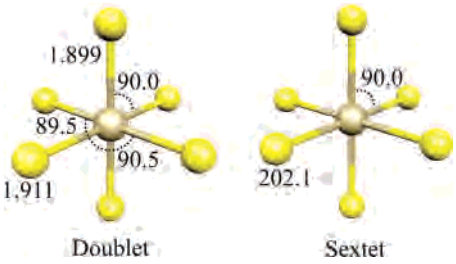

Figure 3. B3LYP-optimized structures for ground and lowest-excited state of AuF_6: (a) doublet ground state (D_{2h}) and (b) lowest-sextet excited state (O_h).

hypersurfaces (cf. Figure 3 for structures). No quartet minimum could be located. At the B3LYP level, the optimized sextet lies 369.6 kJ mol^{-1} above the optimized doublet ground state. This is in agreement with previous HF calculations.[23] The doublet exhibits a slight Jahn−Teller compression of the axial Au−F bonds by 12 pm and a small symmetry breaking in the equatorial plane from D_{4h} to D_{2h}.

Turning finally to Au^{+VII}, we were able to locate only one minimum on the singlet ground-state potential energy surface of d^4 AuF_7, the pentagonal bipyramid (D_{5h}) (Figure 4a; as for AuF_5 above, BP86 calculations lead to a slight puckering of the Au−F bonds within the basal plane; see Supporting Information for detailed coordinates). The lowest vibrational frequency for the D_{5h} minimum is 87 cm^{-1} (B3LYP). At all computational levels used, the two axial Au−F bonds are shorter than the five equatorial ones by 1−3 pm, consistent with some crowding in the equatorial plane (see below). No stable triplet or quintet minima could be located. B3LYP single-point calculations for the triplet and quintet states at the singlet ground-state structure provided excitation energies of 55 kJ mol^{-1} and 127 kJ mol^{-1}, respectively.

Apart from the pentagonal bipyramid, the VSEPR model favors two further coordination polyhedra for heptacoordination,[44] namely, the monocapped trigonal prism (C_{2v}) and the monocapped octahedron (C_{3v}). The monocapped trigonal prism AuF_7 (Figure 4b) is calculated to be a transition state (with an imaginary frequency of 70.3 cm^{-1}). Optimizations of the monocapped octahedral (C_{3v}) structure provided a stationary point with two imaginary frequencies (50.7 and 37.0 cm^{-1}, cf. Figure 4c). At the B3LYP level, the optimized structures for these stationary points are 16.5 (C_{2v}) and 17.2 kJ mol^{-1} (C_{3v}) above the pentagonal bipyramidal minimum.

In view of the existence of AuF_5 as dimer (see above), we have also searched for a $[AuF_7]_2$ dimer structure. However, neither MP2 nor B3LYP optimizations provided indications for a stable dimer.

Vibrational Frequencies. The presumable identification of AuF_7 was based in particular on vibrational spectroscopy. A computational evaluation of the spectrum seems to be a good way to prove or disprove the assignment. Calculated harmonic vibrational frequencies at different computational levels are provided as Supporting Information (Tables S2−S4). As these depend nonnegligibly on computational level, we needed to calibrate the reliability of the frequency calculations. To our knowledge, no IR spectra have been reported, but one Raman spectrum has been reported for $[AuF_5]_2$.[10] B3LYP and MP2 calculations underestimate these Raman frequencies by ca. 20 cm^{-1} (see Supporting Information, Table S5 and Figure S2). BHLYP underestimates the lower frequencies and overestimates the higher frequencies substantially. In particular, the highest Raman frequency is overestimated by 56 cm^{-1} using BHLYP, while the values obtained with B3LYP (11 cm^{-1}) and MP2 (6 cm^{-1}) are closer to the experimental values.

On the basis of this, we rely in the following on the B3LYP data for AuF_7. The vibrational frequency of 734 ± 3 cm^{-1} was assigned to AuF_7 in refs 9 and 20 was not found computationally. The highest computed Au−F stretching frequencies at B3LYP level are 634, 592, and 589 cm^{-1} for the pentagonal bipyramidal (D_{5h}), monocapped trigonal prismatic (C_{2v}), and monocapped octahedral (C_{3v}) stationary points, respectively. The highest frequencies computed for AuF_6 (631 cm^{-1}), AuF_5 (633 cm^{-1}), and $[AuF_5]_2$ (647 cm^{-1}) are also appreciably lower than the 734 cm^{-1} value. Thus, it is unclear at the moment which species has given rise to the reported band.

Reaction Energies for Concerted and Homolytic Elimination. Calculated energies for the elimination reactions $AuF_7 \rightarrow AuF_5 + F_2$ and $AuF_5 \rightarrow AuF_3 + F_2$ are summarized

(44) Hoffmann, R.; Beier, B. F.; Muetterties, E. L.; Rossi, A. R. *Inorg. Chem.* **1977**, *16*, 511−522.

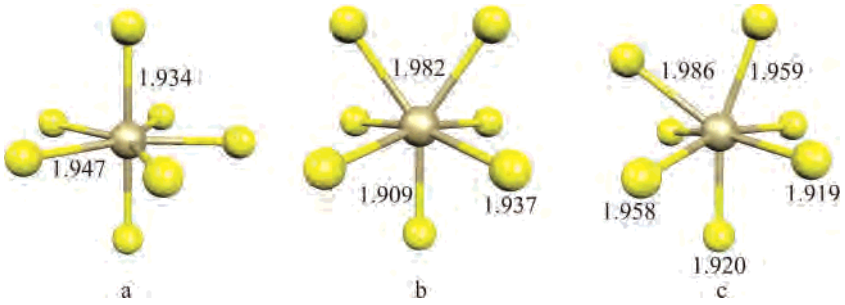

Figure 4. B3LYP-optimized structures of stationary points on the AuF_7 potential energy surface: (a) pentagonal bipyramidal (D_{5h}) minimum, (b) monocapped trigonal prismatic (C_{2v}) transition state, and (c) monocapped octahedral (C_{3v}) stationary point with two imaginary frequencies.

Table 3. Computed Reaction Energies (kJ mol^{-1}) for the Elimination $AuF_{n+2} \rightarrow AuF_n + F_2$ and for the Homolytic Reaction $AuF_{n+1} \rightarrow AuF_n + F$

	HF	MP2	CCSD[b]	CCSD(T)[b]	BP86	BHLYP	B3LYP	*nrel.* B3LYP[d]
				$AuF_7 \rightarrow AuF_5 + F_2$				
D_e	−484.8	−52.6	−234.2	−145.2	−104.4	−268.1	−171.2	−244.2
ZPE	−5.8	−5.4			−5.2	−6.3	−6.4	−4.4
BSSE	−3.5	−30.8			−3.4	−2.3	−5.9	−3.6
sum[a]	−494.0	−88.7			−113.0	−276.7	−183.6	−252.2
				$AuF_5 \rightarrow AuF_3 + F_2$				
D_e	−121.4	124.2	24.2	61.9	101.6	−6.0	49.3	−48.4
ZPE	−8.2	−5.5			−5.1	−6.7	−5.2	−5.2
BSSE	−3.1	−44.6			−4.9	−2.4	−3.7	−8.3
sum[a]	−132.7	74.1			91.7	−15.0	40.5	−61.9
				$AuF_7 \rightarrow AuF_6 + F$				
D_e	−397.6	−10.6	−136.8[c]	−84.5[c]	−101.4		−139.9	
ZPE	−5.0	−2.5			−3.2		−4.9	
BSSE	−2.7	−12.4			−1.4		−1.9	
sum[a]	−397.6	−25.5			−106.0		−146.7	
				$AuF_6 \rightarrow AuF_5 + F$				
D_e	−236.0	103.8	13.1[c]	62.6[c]	213.7		120.7	
ZPE	−8.4	−8.7			−8.0		−7.8	
BSSE	−2.5	−29.4			−2.8		−4.8	
sum[a]	−246.8	65.7			203.0		108.2	

[a] Results including CP and ZPE corrections. [b] No CP correction was possible because of the system size. [c] Single-point calculations at B3LYP-optimized structures. [d] Nonrelativistic ECP for Au used.

Table 4. Calculated Activation Barriers (in kJ mol^{-1}) for the Gas-Phase Elimination of $AuF_7 \rightarrow AuF_5 + F_2$ [a]

input structure	B3LYP	BHLYP	MP2	CCSD[b]	CCSD(T)[b]
B3LYP opt.	24.7	12.9	72.3	27.4	10.0
BHLYP opt.	22.3	40.8	102.1	27.1	5.8

[a] No ZPE and CP corrections are included here. [b] The T_1 diagnostic of coupled-cluster calculations at the transition state are 0.031 at B3LYP-optimized and 0.033 at BHLYP-optimized structures.

in Table 3. Taking the CCSD(T) energy as reference value, CCSD underestimates and MP2 overestimates the elimination energy. This appreciable level dependence of the results indicates a significant influence of nondynamical correlation, as has been discussed previously for Hg^{IV} (d^8) species.[16,18] The comparison of HF and CCSD(T) results shows the tremendous importance of electron correlation for the description of these elimination reactions. In agreement with our previous systematic calibration of DFT methods for the thermochemistry of Hg^{IV} complexes, the B3LYP functional compares well with the CCSD(T) result, whereas the gradient-corrected BP86 provides larger values and the BHLYP functional has lower values. Also, in analogy with the previous studies on Hg^{IV}, the agreement between the B3LYP and CCSD(T) results is expected to improve even further when the larger basis-set dependence of the energies at coupled-cluster than at DFT levels is considered.

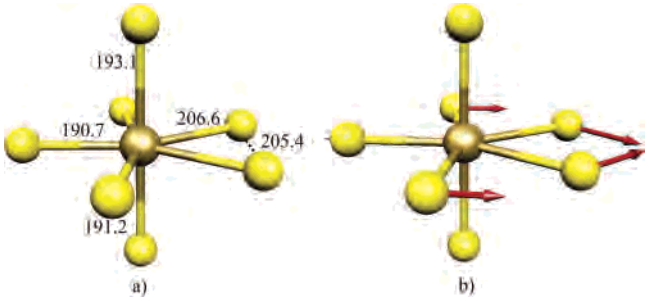

Figure 5. (a) Transition state structure (B3LYP) for the elimination $AuF_7 \rightarrow AuF_5 + F_2$. (b) Indication of the imaginary normal vibrational mode by arrows.

Available computational resources (and the low symmetry of the CP calculations) did not allow a full counterpoise procedure at coupled-cluster levels. CP corrections at the HF and DFT levels tend to lower the reaction energies by ca. 2−6 kJ mol^{-1}. CP corrections at MP2 level are 10 times larger. We expect the coupled-cluster values to be intermediate but closer to the MP2 value. The ZPE corrections are ca. 6 kJ mol^{-1}. There is thus no doubt that the elimination reaction is exothermic by more than 150 kJ mol^{-1}. This renders the existence of AuF_7 unlikely under the conditions reported, unless the system would exhibit unusually high barriers. This does not seem to be the case (see below).

Table 5. Calculated Adiabatic Electron Affinities (in eV) for Hexafluoride Complexes

EA	HF	MP2	CCSD	CCSD(T)	T_1[a]	BP86	B3LYP	exptl
PtF_6 [b] (vertical)[c]	6.50	7.57	7.01	6.68			8.66	
PtF_6 [b]	8.30	6.43	7.43	6.95			6.78	
PtF_6 (1f function)[d]	8.21	6.50	7.48[f]	6.99[f]	0.030 (0.025)	6.02	6.80	7.00 ± 0.35[e]
AuF_6 (1f function)[d]	9.92	8.38	9.01[f]	8.52[f]	0.020 (0.034)	7.15	8.13	
AuF_6	9.85	8.33	8.96[f]	8.47[f]	0.021 (0.034)	7.10	8.06	

[a] T_1 diagnostics (in parentheses for the anion $[MF_6]^-$). [b] Ref 4. [c] Vertical electron affinities. [d] Only one, instead of two, polarization f function was used, with $\alpha = 0.993$, 1.050 for Pt and Au, respectively.[46] This was done for a better comparison with ref 4. [e] Ref 45. [f] Single-point calculations at B3LYP-optimized structures.

We have also studied the successive homolytic splitting of Au−F bonds according to the reactions $AuF_7 \rightarrow AuF_6 + F$ and $AuF_6 \rightarrow AuF_5 + F$ (Table 3). While the bond breaking costs energy for AuF_6, it is actually *exothermic* for AuF_7! How could AuF_7 then still be a minimum on the potential energy surface? A B3LYP calculation of $AuF_6 + F$ at the AuF_7 structure (with one equatorial fluorine atom removed to a large distance) gives an energy 161 kJ mol^{-1} above the AuF_7 minimum. It is thus only the barrier due to structural rearrangement (presumably in the overcrowded basal plane) that renders AuF_7 a local minimum on the potential energy surface. This provides another indication of the extreme instability of Au^{VII}.

Transition States for Elimination Reactions. While the computational location of the true transition state for homolytic bond dissociation in AuF_7 was not successful so far, we have obtained transition states and barriers (Table 4) for the concerted F_2 elimination from AuF_7. Full structure optimization at the coupled-cluster level exceeded the available computational resources in these cases. In addition to full DFT optimizations at theB3LYP and BHLYP levels, we provide single-point MP2, CCSD, and CCSD(T) energies for both the B3LYP- and BHLYP-optimized structures. The transition state exhibits C_{2v} symmetry, with partial formation of an F−F bond in the equatorial plane of AuF_7 (Figure 5a). Indeed, the imaginary vibration of the transition state (Figure 5b) corresponds to the elimination of F_2, combined with the movement of two further equatorial fluorine atoms to give square-pyramidal AuF_5 (cf. Figure 1a).

While the computed activation barriers (Table 4) depend somewhat on the input structure and computational level, they are generally low at both the DFT and coupled-cluster levels (even lower for the latter). We consider the larger MP2 values unreliable in view of the appreciable nondynamical correlation effects (cf. T_1 diagnostics in footnote to Table 4). However, the level dependence is much less pronounced than in previous calculations for the transition states of the related eliminations of Hg^{IV} complexes, $HgX_4 \rightarrow HgX_2 + X_2$ (X = F, Cl). The T_1 diagnostics at the CCSD level of the corresponding transition states were around 0.04−0.06 for elimination from HgF_4 or $HgCl_4$.[18] The values provided here are thus probably more reliable than what is available for those mercury(IV) systems. Together with the exothermic reaction energies (Table 3), this suggests clearly that a stability of AuF_7 up to room temperature, as has been claimed,[9,20,21] is highly unlikely.

Electron Affinities of Hexafluorides. Previous CI calculations predicted an extremely high electron affinity of 9.56 eV for AuF_6,[23] 1.5 eV higher than the value thought to be correct at the time for PtF_6. An extremely large electron affinity had already been assumed for AuF_6 by Bartlett, using simple extrapolation (personal communication cited in ref 24). As the electron affinity is another indicator for the stability of the higher oxidation states, we have computed adiabatic electron affinities for AuF_6 and, for comparison, PtF_6. Our CCSD(T) result of ca. 7.0 eV for platinum hexafluoride agrees well with recent calculations by Schwerdtfeger et al.[4] and with the most recent experimental value[45] (see Table 5; older, still larger values for PtF_6 are considered to be unreliable[4]). Given the good agreement, our computed value of ca. 8.5 eV for AuF_6 should be an accurate prediction. While this is about 1 eV lower than Bartlett's estimate, it remains an extremely large electron affinity and characterizes the hypothetical AuF_6 as one of the most strongly oxidizing species known.

Bonding Comparison of AuF_5 and AuF_7. Figure S3 in Supporting Information compares the frontier Kohn−Sham MOs for AuF_7, $[AuF_6]^{-1}$, and AuF_5. Consistent with the high oxidation state of the heptafluoride, the highest-occupied MOs are essentially π-type lone pairs on the axial ligands, with only weak metal−ligand antibonding character. In AuF_5, the three highest-occupied MOs derive from the t_{2g} set of octahedral $[AuF_6]^{-1}$ (cf. Figure S3c) and exhibit somewhat more pronounced π-antibonding character. The character of the very low-lying virtual orbitals (Figure S3b) allows us to understand clearly why this Au^V species prefers to exist as a dimer (or trimer). The relatively respectable HOMO−LUMO gaps of AuF_7 and $[AuF_6]^-$ explain why they exhibit closed-shell singlet ground states and relatively high excitation energies.

4. Conclusions

This quantum-chemical study has shown that the experimental observation of AuF_7 reported about 20 years ago is highly improbable. The previously reported, so far unreproduced experimental characterization of gas-phase AuF_7 by an IR band at 734 ± 3 cm^{-1} was not confirmed by our calculations. The computed, strongly exothermic elimination of F_2 with a low activation barrier is not consistent with the reported stability of AuF_7 up to room temperature, and even

(45) Korobov, M. V.; Kuznetsov, S. V.; Sidorov, L. N.; Shipachev, V. A.; Mit'kin, V. N. *Int. J. Mass Spectrom. Ion Processes* **1989**, *87*, 13−27.

(46) Ehlers, A. W.; Bohme, M.; Dapprich, S.; Gobbi, A.; Hollwarth, A.; Jonas, V.; Kohler, K. F.; Stegmann, R.; Veldkamp, A.; Frenking, G. *Chem. Phys. Lett.* **1993**, *208*, 111−114.

the existence at liquid-nitrogen temperature is doubtful. Moreover, even the homolytic dissociation of one equatorial Au−F bond is exothermic and has a barrier only from structural rearrangement. If at all, such a high-energy species will only be accessible in more sophisticated matrix-isolation or mass-spectrometry experiments. In view of the extremely high electron affinity of AuF_6, this Au^{VI} species is also unlikely to exist at most experimentally viable conditions. Oxidation state +V thus remains the highest oxidation state for the group 11 element gold that is known beyond doubt.

Acknowledgment. We are grateful to M. Straka and R. Reviakine for comments and technical assistance and to A. Patrakov for the translation of Russian literature.

Supporting Information Available: BP86-optimized minimum structures for AuF_5 and AuF_7 (Table S1), harmonic vibrational frequency analysis (Table S2−S4), comparison of computed and experimental Raman frequencies and intensities for $[AuF_5]_2$ (Table S5), cartesian coordinates (in Å) of optimized structures for $Au^{+V,VI,VII}$ complexes (Table S6−S8), BP86-optimized structures for the singlet ground states of AuF_5 and AuF_7 (Figure S1), Raman frequencies for $[AuF_5]_2$ at the B3LYP, BHLYP, and MP2 levels compared with experimental results (Figure S2), Kohn−Sham molecular orbitals of AuF_7 (D_{5h}), AuF_5 (D_{3h}), and $[AuF_6]^{-1}$ (O_h) at the B3LYP level (Figure S3). This material is available free of charge via the Internet at http://pubs.acs.org.

IC051944Y